Synthesis of a magnetic polystyrene-based cation-exchange resin and its utilization for the efficient removal of cadmium (II)

Zhaohe Wang, Shilei Ding, Zhixia Li, Fuwei Li, Tingting Zhao, Jiangfeng Li, Hongfei Lin and Congjin Chen

ABSTRACT

A magnetic cation-exchange resin (MCER) was prepared by copolymerization of oleic acid-grafted magnetite with styrene, divinylbenzene (DVB), and triallylisocyanurate (TAIC) for removing Cd(II) from wastewater. A non-magnetic cation-exchange polystyrene resin (CEPR) was also prepared as a reference. Structural and morphological analyses revealed that the MCER and CEPR were mesoporous microspheres; the MCER contained about 25% Fe_3O_4. The influence of temperature, pH, contact time, and the initial concentration of Cd(II) on the adsorption of Cd(II) was investigated. The maximum adsorption capacity of the MCER reached 88.56 mg/g, which was achieved at 343 K using a Cd(II) initial concentration of 200 mg/L. The adsorption processes attained equilibrium within 120 min for the MCER and 300 min for the CEPR, and were well described by a pseudo-second-order kinetic model. Furthermore, the equilibrium adsorption data fitted the Freundlich isotherm model better than the Langmuir model. The superior magnetic response and regeneration of the MCER make it a good candidate as an adsorbent for removing Cd(II) from wastewater.

Key words | adsorption, cadmium ion, magnetic cation-exchange resin, polystyrene microsphere, wastewater

Zhaohe Wang
Shilei Ding
Zhixia Li (corresponding author)
Fuwei Li
Tingting Zhao
Jiangfeng Li
Congjin Chen
School of Chemistry and Chemical Engineering,
Guangxi University,
Nanning 530004,
China
E-mail: *zhixiali@hotmail.com*;
zhixiali@gxu.edu.cn

Hongfei Lin
Guangxi Bossco Environmental Protection Technology Co., Ltd,
Nanning 530007,
China

INTRODUCTION

With rapid economic growth and industrial development, water pollution is becoming an increasingly serious problem. Heavy metal pollution, especially that caused by the electroplating and metal finishing industries, has become an important source of water pollution (Järup 2003; Naser 2013). Even low concentrations of heavy metals can cause great harm to human health because of their non-biodegradability and bioaccumulation (Fu & Wang 2011; Barton *et al.* 2016). Among the harmful heavy metals, Cd is extremely toxic as it can produce effects in the kidneys, liver, lungs, and immune system, and has been shown to damage DNA (Benbrahim-Tallaa *et al.* 2009; Morales *et al.* 2016). For instance, 1.33 million fish fry and 40,000 kg of fish were killed in a Cd pollution incident in the River Guangxi Longjiang in 2012. Therefore, the search for safe and economical methods to treat Cd wastewater is one of the most important tasks in the field of pollution control.

The main methods currently used in this regard by many industries are chemical precipitation and electrochemical reduction (Martinez *et al.* 2012; Tao *et al.* 2014). These chemical methods are effective, but cannot achieve complete removal of heavy metals; furthermore, the chemicals involved in these methods can become a new pollution source (Barakat 2011). Physical methods such as adsorption, membrane separation, and ion exchange have been extensively studied in recent years because of the good adsorbability of heavy metals and the easy regeneration and environmentally friendly properties of membranes and resins (Guo *et al.* 2012; Liang *et al.* 2013; Li *et al.* 2016). Bazargan prepared a sodium diimidoacetate-based chelating resin (D401) with great potential for Zn^{2+} removal (Bazargan *et al.* 2017). In another study, polydopamine nanoparticles with an average diameter of 75 nm were prepared for the selective removal of Cu(II), and the maximum adsorption capacity was 34.4 mg/g (Farnad *et al.* 2012).

Recently, the application of magnetic polymer adsorbents for the removal of heavy metal ions has become a new topic of research. Magnetic polymer adsorbents

doi: 10.2166/wst.2018.239

combine several advantages, including rapid and facile separation from the reaction medium upon the application of a magnetic field, a separation process without the generation of secondary waste, and the use of materials that are recyclable and easily reusable (Bagheri *et al.* 2012). Li *et al.* prepared a novel magnetic cation-exchange resin via suspension polymerization and hydrolysis that exhibited high adsorption capacities for Cu(II) and Ni(II) (Li *et al.* 2017). In Shen's research, magnetic polymeric particles were functionalized with tetraethylenepentamine (TEPA-NMPs), and were used for the removal of Cr(VI) (Shen *et al.* 2013). The results showed that Cr(VI) could be effectively adsorbed on TEPA-NMPs by electrostatic attraction. The target and challenge for the application of a magnetic polymer adsorbent is to develop a new type of ion-exchange resin with high capacity and magnetic response.

With regard to Cd(II) removal from wastewater, lignin-based ion-exchange resins were developed by polymerization of sodium lignosulfonate and glucose (Liang *et al.* 2013) or polymerization of calcium lignosulfonate and formaldehyde (Fu *et al.* 2016), and the obtained resins achieved an adsorption capacity for Cd(II) of 17.93 mg/g and 92.15 mg/g, respectively. A chelated ion-exchange resin prepared by condensing *p*-hydroxybenzoic acid and formaldehyde was used for adsorption of metal ions, and the adsorption capacity for Cd(II) was 1.591 mmol/g (Bhatt *et al.* 2012). In addition, D-401 resin was used for adsorption of Cd(II), and the maximum adsorption capacity reached 2.20 mmol/g resin (Wong *et al.* 2014). The adsorption capacity was strongly dependent on the Cd(II) initial concentration, pH, temperature and physicochemical characteristics of the adsorbents. Although ion-exchange resins have been widely studied for the recovery of Cd(II), little work has been done to develop magnetic ion-exchange resins to treat Cd(II) wastewater.

In this study, magnetic and non-magnetic cation-exchange polystyrene resins were prepared by the suspension polymerization method. The performance of the obtained resins for removing Cd(II) ions from wastewater was investigated. The adsorption kinetics and isotherms are discussed. Furthermore, the regeneration performance of the obtained resins was studied.

MATERIALS AND METHODS

Materials

Styrene (St, AR), divinylbenzene (DVB, 55%), triallylisocyanurate (TAIC, AR) and dibenzoyl peroxide (BPO, AR) were obtained from Shanghai Mclean Biochemical Technology Co. Ltd, China. $FeCl_3{\cdot}6H_2O$, $FeCl_2{\cdot}4H_2O$, polyvinyl alcohol (PVA) and polyvinylpyrrolidone (PVP) were of analytical grade and purchased from Guangzhou Jinhua Da Chemical Reagent Co., Ltd. Oleic acid (OA), toluene and heptane were of analytical grade and obtained from Chengdu Kelong Chemical Reagent Factory. St was purified before use according to the following procedure: it was washed with 10% NaOH solution, dried using anhydrous sodium sulfate, and finally vacuum distilled in a rotary evaporator at 75 °C. Deionized water was used throughout the study.

Synthesis of cation-exchange resins

A cation-exchange polystyrene resin (CEPR) was synthesized by suspension polymerization. St (5.0 g), DVB (1.0 g), and TAIC (0.5 g) as the monomers, BPO (0.1 g) as the initiator, and toluene (4 mL) and heptane (3 mL) as the porogens were mixed to form the organic phase. Deionized water (80 mL), PVA (0.4 g), PVP (0.4 g), and 3–4 drops of methylthionine chloride solution (5%) were mixed to form the aqueous phase. The organic and aqueous phases were transferred into a 250 mL stainless steel reactor (Figure 1). After the gas in the reactor was replaced three times with nitrogen, the reactor was filled with nitrogen at 2.5 atm, heated to 80 °C and maintained at this temperature for 2.5 hours. Then the reactor was further heated to 90 °C and maintained at this temperature for another 2.5 hours. The whole process proceeded with a stirring rate of 500 rpm. The resultant precursor resin was alternately washed with hot and cold water, and dried at 55 °C in a vacuum drying oven. The obtained resin (3 g) was added to sulfuric acid (98%, 25 mL) and sulfonated at 60 °C for 8 hours. The final particles were washed with water and ethanol, and dried at 55 °C in a vacuum drying oven.

The magnetic cation-exchange resin (MCER) was prepared by a two-step method. First, oleic acid-grafted

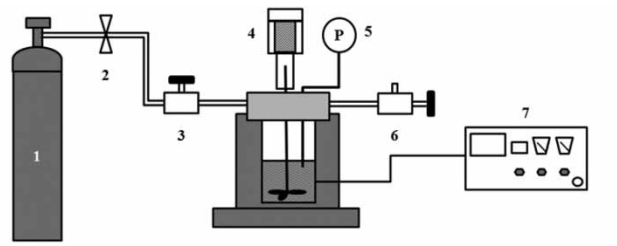

1. N_2 bottle; 2. relief valve; 3. intake valve; 4. magnetic stirrer; 5. pressure gauge; 6. exhaust valve; 7. temperature and agitation controller

Figure 1 | Diagram of the experimental apparatus.

magnetite (OA-Fe_3O_4) was prepared as follows. $FeCl_2{\cdot}4H_2O$ (4.12 g) and $FeCl_3{\cdot}6H_2O$ (10.61 g) were dissolved in HCl (200 mL) in a flask (pH = 1.72). When the flask was heated to 80 °C, 60 mL of diluted ammonia water was added to the mixed Fe^{2+}/Fe^{3+} solution slowly under stirring in a N_2 atmosphere (final pH = 10.46), and left to react for 30 min. OA (0.8 g) was then added into the flask, and the flask was heated to 90 °C and left to react for 120 min. The resultant particles (OA-Fe_3O_4) were washed with ethanol and deionized water, and dried at 55 °C in a vacuum drying oven. Next, 2.0 g of OA-Fe_3O_4 was dispersed in the organic phase (the same as for the preparation of CEPR), and agitated for 30 min by ultrasonication. The aqueous phase consisted of deionized water (80 mL), PVA (1.0 g), PVP (1.0 g), and methylthionine chloride solution (5%, 3–4 drops). The ultrasonically treated organic phase and the aqueous phase were transferred to a stainless steel reactor and left to react under the same conditions as those used for the preparation of CEPR. The obtained dark-brown particles were dried and sulfonated by the same method as that used for the CEPR. The polymerization scheme for the preparation of MCER is shown in Figure 2.

Analytical methods

The obtained resins were characterized by Fourier transform infrared (FTIR) spectroscopy (8400S, Shimadzu, Japan), scanning electron microscopy (SEM) (S-3400N, Hitachi, Japan), powder X-ray diffraction (XRD) (SmartLab3, Rigaku, Japan), thermogravimetric analysis (TGA) (209F3, NETZSCH, Germany), Brunauer-Emmett-Teller (BET) surface area measurements (NOVA 2200e, Quantachrome, USA). The adsorption behavior for Cd(II) ion on the obtained resins was characterized by polarographic analyzer (JP-303, Chengdu Instrument Factory, China).

Adsorption of Cd(II) ions

A stock solution of Cd(II) (1,000 mg/L, 500 mL) was prepared by dissolving CdO (0.5712 g) in deionized water. Ten milliliters of 6 *M* HCl were added to stabilize the Cd(II) ions in solution. The Cd(II) stock solution was diluted to different concentrations (10, 20, 40, 60, 80, 100, 120, 140, 160, and 200 mg/L) using deionized water to obtain simulated Cd(II) wastewater. First, batch experiments were conducted using 10 mL of the Cd(II) solution with a concentration of 100 mg/L to determine the effects of pH, temperature, and contact time on the adsorption of Cd(II). After the pH of the solution was adjusted to a desired value using both 1 *M* HCl and 1 *M* NaOH, 20 mg of the resin was added to the solution. The resultant suspensions were agitated for a specified time by using a shaker, and then separated and analyzed by polarography. Then, the effect of the initial concentration of Cd(II) on the adsorption performance of the resins was investigated at pH 3 for a contact time of 12 hours using 10 mL of the Cd(II) solution with different initial concentrations. The adsorption capacity (*Q*) and removal efficiency (*E*) were calculated according to Equations (1) and (2), respectively:

$$Q(mg/g) = \frac{V(C_0 - C_e)}{M} \quad (1)$$

$$E(\%) = \frac{(C_0 - C_e)}{C_0} \times 100 \quad (2)$$

where *V* is the volume of the Cd(II) solution (L), *M* is the weight of the resin (g), and C_0 and C_e are the initial and final equilibrium concentrations of Cd(II) in the solution (mg/L), respectively.

Desorption and regeneration experiments

To investigate the reusability of the obtained resins, desorption and regeneration experiments were conducted at

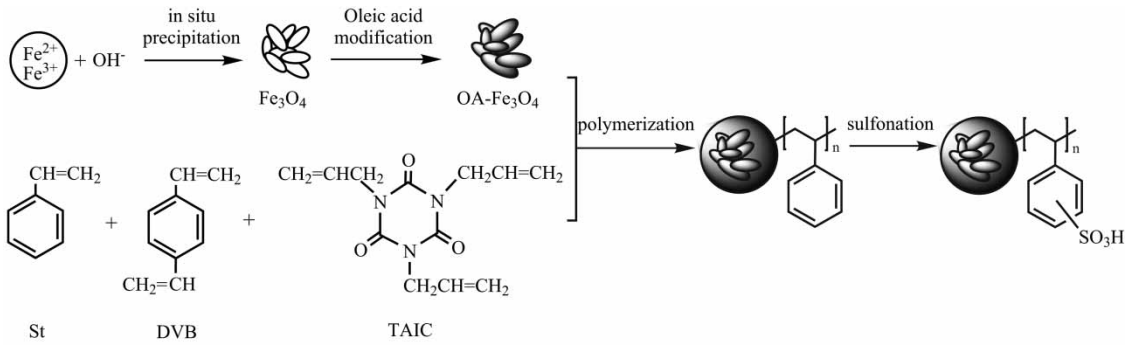

Figure 2 | Polymerization scheme for the preparation of the MCER.

room temperature. For the desorption studies, the Cd-loaded resins were dispersed in 10 mL of a 0.1 *M* HCl solution and left to stand for 12 hours. After desorption, the resins were repeatedly washed with deionized water and then dried for reuse. Six consecutive adsorption-desorption cycles were conducted for each kind of resin, and in each cycle, the initial Cd(II) ion concentration was 100 mg/L, resin dosage was 20 mg and Cd(II) solution was 10 mL. The adsorption-desorption cycle efficiency (R) was calculated using Equation (3).

$$R(\%) = \frac{Q_n}{Q_0} \times 100 \quad (3)$$

where Q_o is the initial adsorption capacity of the resins (mg/g), and Q_n is the adsorption capacity of the resin after desorption for n-times.

RESULTS AND DISCUSSION

Characterization of the cation-exchange resins

Figure 3(a) illustrates the process for the separation of the MCER under a magnetic field. It indicates that the resin incorporating the magnetite particles can be easily separated by exposing it to an external magnetic field. The XRD pattern of the MCER is presented in Figure 3(b) and compared with that of pure Fe_3O_4 particles. Obvious diffraction peaks appear at $2\theta = 30.390°$, 35.640°, 43.251°, 57.250° and 62.831°, which correspond to the planes (220), (311), (400), (511), and (440), respectively, of the inverse spinel structure of Fe_3O_4. This is consistent with the face cubic structure of Fe_3O_4 with standard values (JCPDS file no. 16–629) (Davarpanah *et al.* 2015). This demonstrates the existence of Fe_3O_4 particles within the MCER matrix.

The thermal stabilities of the CEPR and MCER were examined by TGA, and the results are shown in Figure 3(c). The slight weight loss observed in the temperature range 30–100 °C is mainly attributed to the loss of water. The weight losses for the two resins between 100 and 370 °C are about 15%, mainly resulting from the thermal decomposition of the non-crosslinked areas of the resins. Rapid weight losses are observed from 370 to 450 °C, along with sharp peaks in the DTG curves at about 430 °C, which are mainly due to the thermal decomposition of the crosslinked areas of the resins. The total weight loss of the MCER is significantly lower than that of the CEPR, mainly due to the existence of Fe_3O_4 particles in the former. The content of Fe_3O_4 in the MCER estimated by comparing the weight losses of the CEPR and MCER at 500 °C is about 25%.

Figure 4 shows the SEM images of the resultant resins. Both CEPR and MCER exist as spherical beads, with grain sizes of approximately 180–300 μm, which is 2–3 times smaller than those of the conventional resins. Numerous small granular bulges are observed on the surface of MCER, which are mainly due to the embedding of the agglomerated Fe_3O_4 particles. As shown in Table 1, the average pore diameters of the CEPR and MCER are 3.7 and 4.05 nm, respectively, indicating that the resultant resins are mesopore-predominant materials. Specific surface area and total pore volume also slightly changed with the incorporation of Fe_3O_4 particles. OA-Fe_3O_4 can combine with St and/or DVB through a polymerization reaction with the double bonds, as indicated in Figure 2. The Fe_3O_4 particles and the long aliphatic chains on OA could weaken the polymerization reaction between the three monomers (St, DVB and TAIC), leading to a looser structure for the MCER. This is likely responsible for the slightly larger pore diameter and volume observed in the MCER. The pore properties are closely associated with the Cd(II) adsorbability of the resins.

Figure 5 shows the FTIR spectra of OA-Fe_3O_4, CEPR, and MCER, which are compared with those of pure Fe_3O_4. The obvious adsorption bands at 2922.3 and 2848.1 cm^{-1}, identified as the stretching vibrations of $-CH_3$ and $-CH_2$, were observed for OA-Fe_3O_4, but not for Fe_3O_4, indicating that OA is successfully bonded to Fe_3O_4. The broad stretching band near 3,500–3,000 cm^{-1} in the OA-Fe_3O_4 spectrum is mainly due to adsorbed water and the O – H bonds in Fe_3O_4 (Lee *et al.* 2010). As seen from Figure 5(b), a broad stretching band near 3,700–3,100 cm^{-1} and an obvious adsorption peak at 1,640.2 cm^{-1} are observed in the case of the MCER. The former is attributed to the O – H stretching vibrations of the adsorbed water, and the latter is likely due to the antisymmetric stretching vibrations of C = O in oleate. The adsorption peak of polystyrene at 536.2 cm^{-1} in the CEPR spectrum shifts to 565.1 cm^{-1} in the MCER spectrum, which is due to the overlap with the adsorption band of Fe – O in Fe_3O_4. These results indicate that OA-Fe_3O_4 is successfully embedded into the styrene-based polymer matrix. The attached sulfonyl groups of the CEPR were identified with the obvious stretching band of S = O in the range 1,300−1,000 cm^{-1} (Lee *et al.* 2010). The S = O bands are enhanced for the MCER, indicating that more sulfonyl groups are bonded to the MCER.

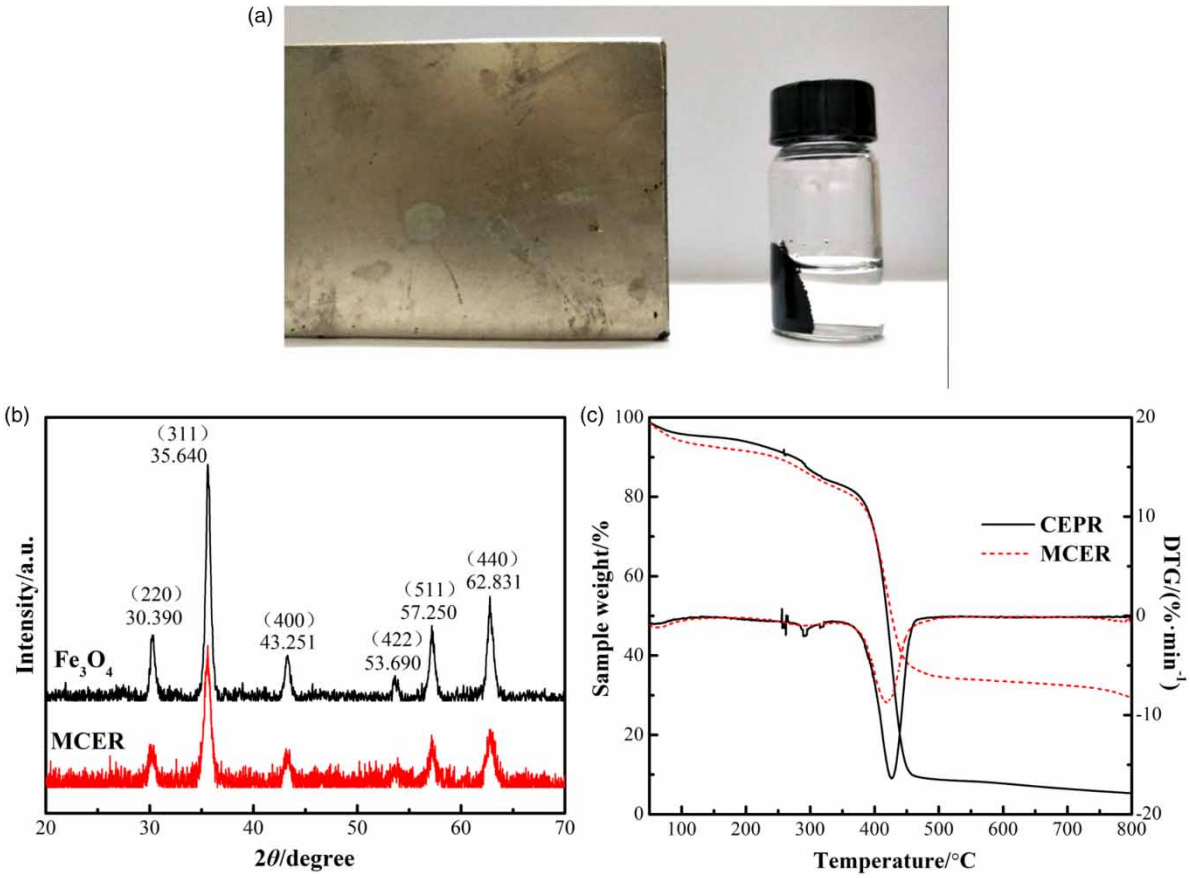

Figure 3 | (a) Separation of MCER under an external magnetic field. (b) X-ray powder diffractogram of Fe_3O_4 and MCER. (c) TGA curves of the CEPR and MCER.

Adsorption of Cd(II) ions from aqueous solutions

Effect of solution pH

According to previous studies, pH is an important factor affecting the adsorption behavior of sorbents for heavy-metal ions because of its effect on the surface charge of the sorbent and the conversion of the metal ion species (Yu *et al.* 2012). The effect of pH on the adsorption of Cd(II) by the obtained resins was studied in the pH range 2.0–6.0 using a Cd(II) aqueous solution with an initial concentration of 100 mg/L. As presented in Figure 6(a), at the tested pH range, the equilibrium adsorption capacities of the two resins remains at about 43 mg/g, and is not significantly affected by pH. This indicates that the resultant resins are favorable for the treatment of Cd(II)-containing wastewater over a wide pH range. However, it has been reported that a high pH, e.g., higher than 6.0, could lead to the formation of $Cd(OH)_2$, involving Cd(II) and OH^- (Liang *et al.* 2013). Therefore, to eliminate the effect of metal precipitation, all further adsorptions of the Cd(II) ions were performed at the pH value of 3.

Effect of contact time

The adsorption of Cd(II) ions on the two resins as a function of contact time was studied at different temperatures. The contact time was varied in the range 1–480 min. As can be seen in Figure 6(b), as the contact time increased, the adsorption capacity (Q) increased, until equilibrium was reached. The adsorption of Cd(II) on the MCER was rapid and attained equilibrium within 120 min, whereas the adsorption on the CEPR attained equilibrium only within 300 min. The final equilibrium values of Q for the two resins were very similar, and increased with increasing temperature. These results indicate that adsorption of Cd(II) on the two resins is an endothermic reaction. The MCER achieved the adsorption equilibrium faster, probably due to its superior hydrophilicity, as evidenced by the presence of many O – H groups on its surface (Figure 5). The larger pores of

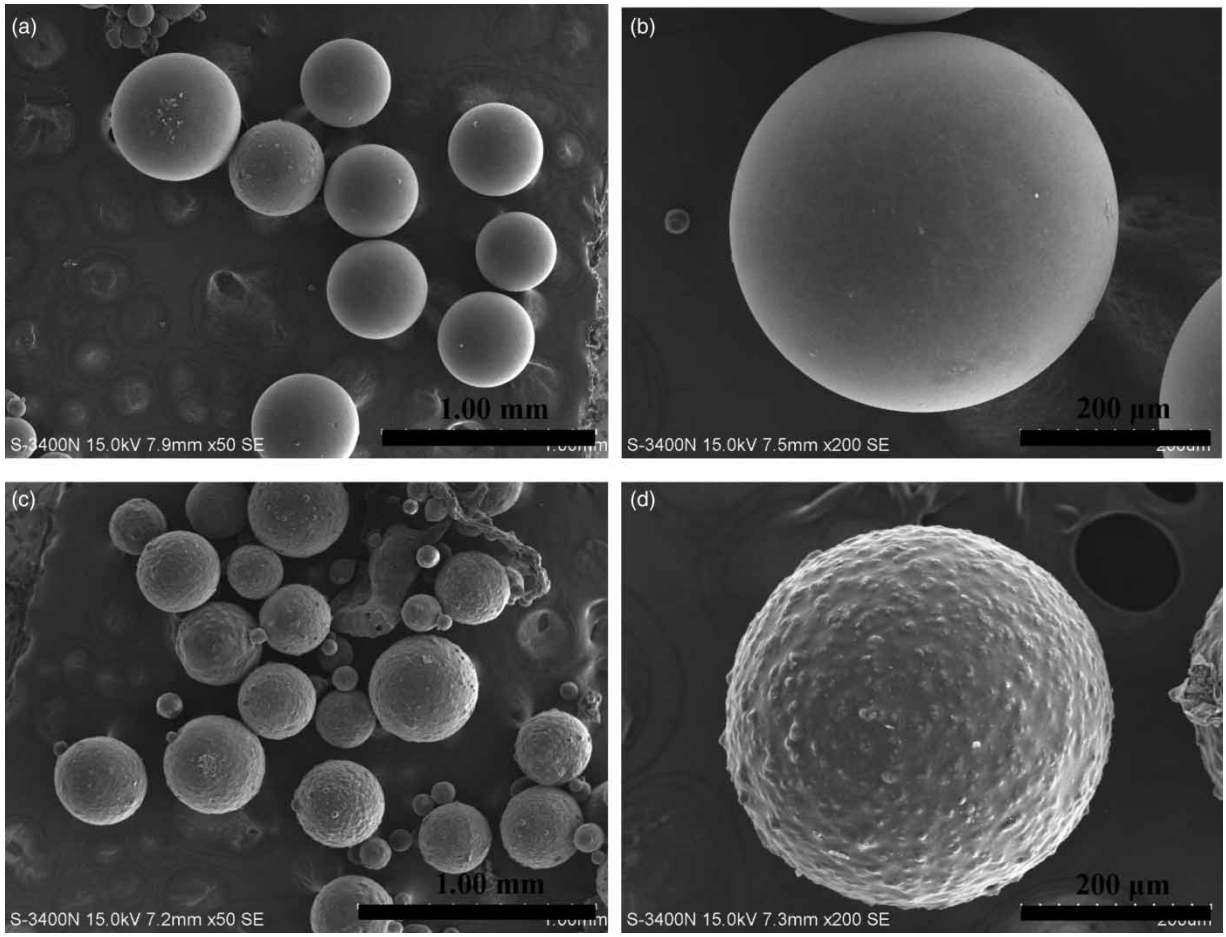

Figure 4 | SEM images of CEPR (a), (b) and MCER (c), (d).

the MCER (Table 1) could help to decrease the diffusion resistance and shorten the adsorption time of Cd(II).

Effect of the initial concentration of Cd(II)

Figure 6(c) and 6(d) show the effect of Cd(II) initial concentration on the adsorption capacity (Q) and removal efficiency (E) of Cd(II). As the initial concentration increases, the Q values of the two resins increase linearly, whereas the E values gradually decrease. The maximum adsorption capacities of the CEPR and MCER in the tested concentration range are 88.51 mg/g and 88.56 mg/g, respectively. The adsorption amount increased slightly with temperature, indicating the endothermic nature of Cd(II) adsorption on the CEPR and MCER. As seen in Figure 6(d), the E values for the two resins are higher than 90% when the adsorption experiments were carried out at 323 K or 343 K, with the Cd(II) concentration ranging from 10 to 100 mg/L. This indicates that the two resins are effective absorbents for treating wastewater with low concentrations of Cd(II). These results demonstrate that the incorporation of Fe_3O_4 in the polystyrene resin did not affect the adsorption capacity of the CEPR. In actual application for the treatment of wastewater, which would likely contain a higher concentration of Cd(II), increasing the dosage of the resins and temperature would help to achieve the effective removal of Cd(II) ions.

Table 1 | Physicochemical properties of resins

Resins	Specific surface area (m^2/g)	Average pore diameter (nm)	Total pore volume (cm^3/g)	Functional group
CEPR	165.5	3.70	0.154	$-SO_3H$
MCER	164.3	4.05	0.162	$-SO_3H$

Analysis of adsorption kinetics

The adsorption kinetics of Cd(II) was studied to elucidate the adsorption behaviors of the two resins. Several kinetic models were used to test the experimental data. The

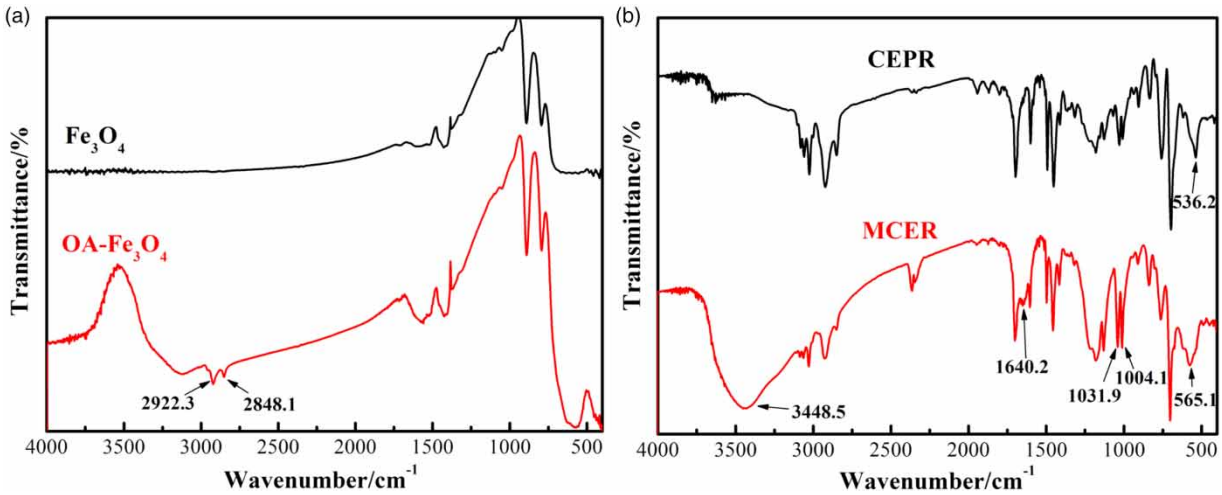

Figure 5 | FTIR spectra of Fe_3O_4, OA-Fe_3O_4 (a) and two cation-exchange resins: CEPR and MCER (b).

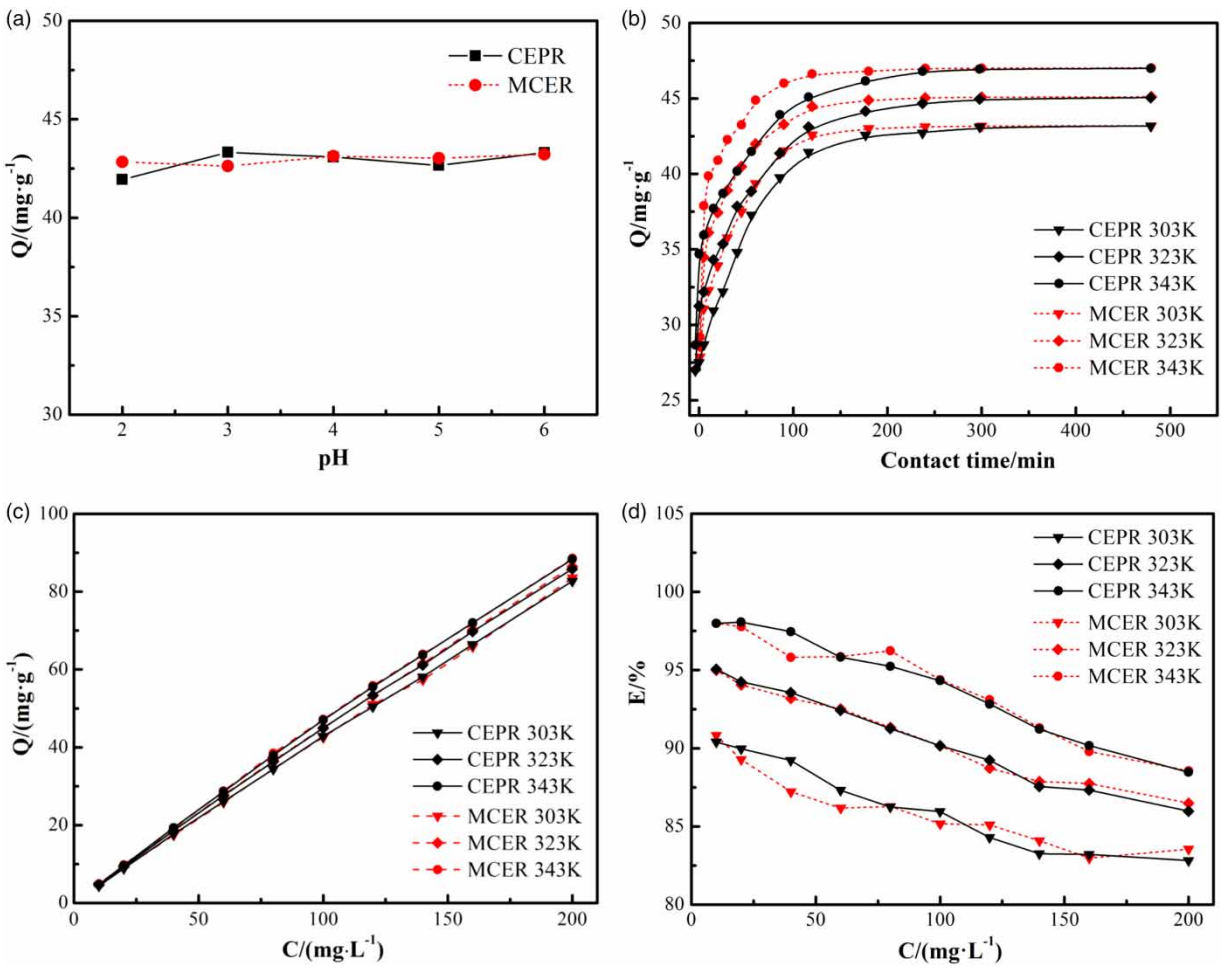

Figure 6 | The effect of pH (a) and contact time (b) on adsorption of Cd(II) on CEPR and MCER; and the effect of Cd(II) initial concentration on the adsorption capacity (c) and removal efficiency (d) of Cd(II).

pseudo-first-order kinetic equation is given as Equation (4) (Pan *et al.* 2012):

$$\log(Q_e - Q_t) = \log Q_e - \frac{k_1 t}{2.303} \quad (4)$$

and the pseudo-second-order equation is expressed as follows (Plazinski *et al.* 2013):

$$\frac{t}{Q_t} = \frac{1}{k_2 Q_e^2} + \frac{t}{Q_e} \quad (5)$$

where Q_e and Q_t are the adsorption capacities at equilibrium and time t (min) (mg/g), respectively, k_1 is the pseudo-first-order rate constant (1/min), and k_2 is the pseudo-second-order rate constant (mg/(g min)).

Furthermore, the intraparticle diffusion model can be described as (Wu *et al.* 2009):

$$Q_t = k_p t^{0.5} \quad (6)$$

where k_p is the rate constant (mg/(g·min$^{1/2}$)), which can be obtained from the plot of Q_t against $t^{0.5}$.

The data for the adsorption capacity with contact time (shown in Figure 6(b)) were tested against these three kinetic models. The results are presented in Figure 7. The regression coefficient (R^2) values, the predicted Q_e values, and the rate constants of the three kinetic models (k_1, k_2, and k_p) are listed in Table 2. It can be clearly seen that the fit of the pseudo-second-order curve is the best, and the values of R^2 for the pseudo-second-order are higher than those of the other kinetic models. Moreover, the Q_e values of Cd(II) predicted by the pseudo-second-order model are very close to the experimental values (Q_{exp}). Therefore, the adsorption of Cd(II) on the two resins can be best described by the pseudo-second-order kinetic model, implying that the adsorption of Cd(II) on the obtained resins is an ion-exchange process (Kara *et al.* 2015).

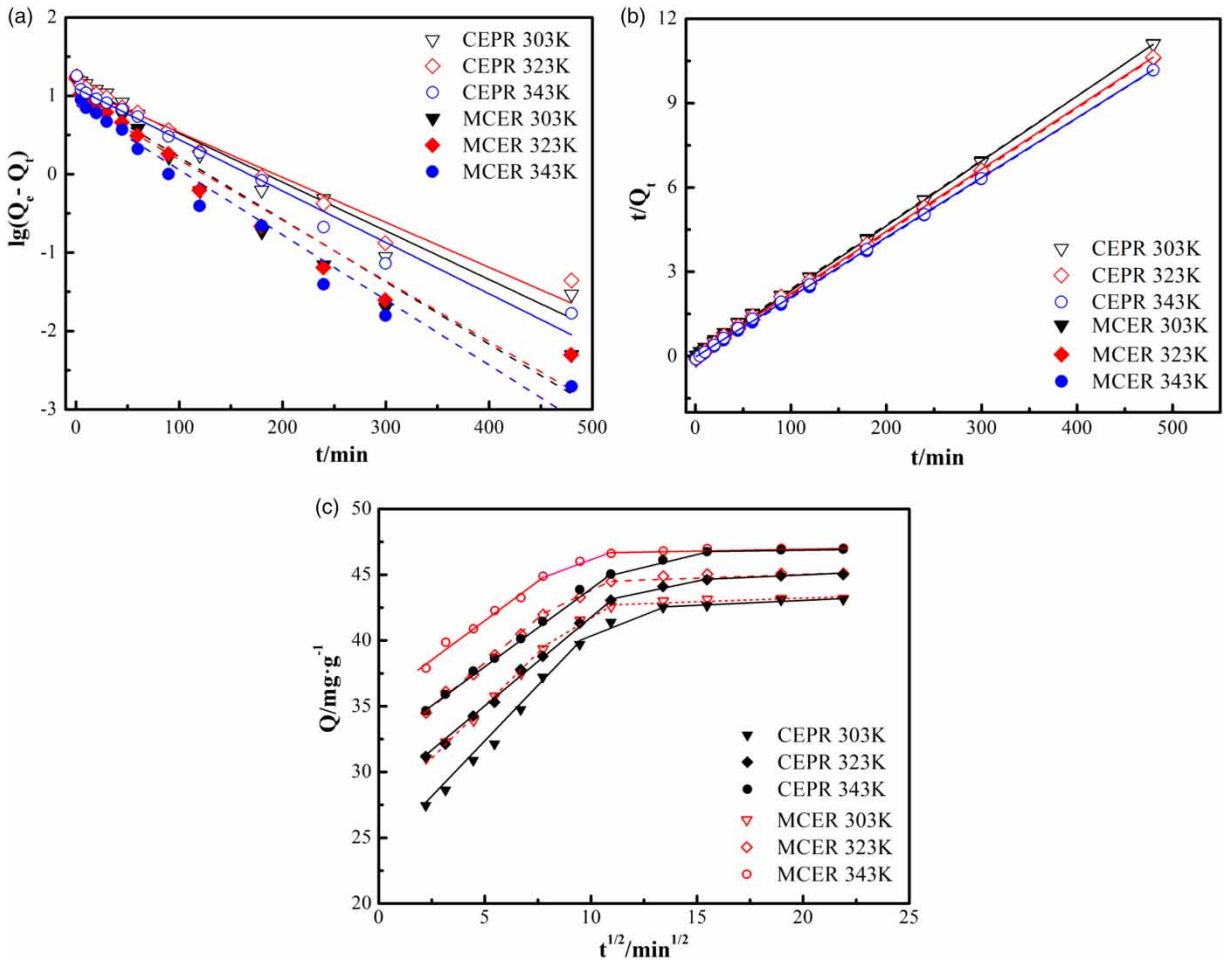

Figure 7 | Adsorption kinetics of Cd(II) on CEPR and MCER, (a) pseudo-first-order model, (b) pseudo-second-order model, (c) intraparticle diffusion plot.

Table 2 | Kinetic adsorption parameters for Cd(II) adsorbed on the two resins

			Pseudo-first-order model			Pseudo-second-order model			Intraparticle diffusion	
Resins	**T (K)**	**Q_{exp}**	**$k_1(10^{-2})$**	**Q_e**	**R^2**	**$k_2(10^{-3})$**	**Q_e**	**R^2**	**k_p**	**R^2**
CEPR	303	43.19	1.430	14.06	0.9651	3.504	43.78	0.9995	0.851	0.7974
	323	45.09	1.322	13.09	0.9706	3.423	45.64	0.9994	0.752	0.8281
	343	47.01	1.508	12.72	0.9781	4.159	47.48	0.9996	0.660	0.8341
MCER	303	43.19	1.833	10.35	0.9537	5.451	43.67	0.9997	0.639	0.7405
	323	45.11	1.780	9.28	0.9607	6.585	45.47	0.9998	0.537	0.7458
	343	47.02	1.191	7.84	0.9659	8.999	47.30	0.9999	0.436	0.7059

Based on the curves of Q_t and $t^{0.5}$ (shown in Figure 7(c)), the adsorption behavior of Cd(II) on the two resins at different temperatures can be described by three linear portions. The first portion, with a steep slope, indicates a rapid diffusion stage, in which the Cd(II) ion is absorbed rapidly by the sulfonic acid group. In the second portion, the Cd(II) ions gradually enter the inside of the resin matrix and are adsorbed onto the inner active sites. The third portion, where the slope is close to zero, indicates that the equilibrium state has been reached. Since the straight line for the first portion does not pass through the origin, intraparticle diffusion is not the rate-determining step for Cd(II) adsorption (Li *et al.* 2017). The film diffusion of the Cd(II) ion (through the boundary layer that surrounds the resin particles) likely controls the adsorption process (Khambhaty *et al.* 2009).

Analysis of adsorption isotherms

Adsorption isotherm analysis is important for describing the relationship between equilibrium adsorption capability and the equilibrium concentration of the metal ions in solution. In order to better evaluate the adsorption capacity of an adsorbent and comprehend the interaction between the adsorbent and adsorbate, the Langmuir and Freundlich isotherm models were applied to simulate the experimental data.

The Langmuir isotherm is given as (Chen 2015):

$$\frac{C_e}{Q_e} = \frac{C_e}{Q_m} + \frac{1}{Q_m b} \tag{7}$$

where C_e is the residual concentration of Cd(II) in solution (mg/L), Q_m is the maximum adsorption capacity of Cd(II) (mg/g), and b is the Langmuir constant related to the affinity of the binding sites (L/mg).

The Freundlich model can be described by Equation (8) (Millar *et al.* 2016):

$$Q_e = K_F C_e^{1/n} \tag{8}$$

or its logarithmic form:

$$\log Q_e = \log K_F + \frac{1}{n}\log C_e \tag{9}$$

where K_F is a constant relating to the adsorption capacity (mg/g) and $1/n$ is an empirical constant related to the adsorption intensity. The values of K_F and $1/n$ are calculated from the slope and intercept of the plot of $\log Q_e$ versus $\log C_e$. The $1/n$ values of the Freundlich model can indicate the type of isotherm. For $0 < 1/n < 1$, the adsorption of adsorbate onto adsorbent is favorable. A higher value of n means stronger adsorption intensity.

The experimental data from the two resins were fitted to the Langmuir and Freundlich models, and the results are shown in Figure 8. The isotherm parameters are presented in Table 3. As shown, the curves of the Freundlich model fit better than those of the Langmuir model. The correlation coefficients for the Langmuir isotherm model are all higher than 0.83, but the values are better for the Freundlich isotherm, with R^2 higher than 0.97, demonstrating that the Freundlich isotherm model is more suitable for describing the adsorption behavior. This indicates that the adsorption of Cd(II) on the two resins is a multilayer adsorption process on the heterogeneous resin surface (Li *et al.* 2017). In addition, the $1/n$ values for the Freundlich adsorption isotherms of the CEPR and MCER are lower than 1, implying that the adsorption of Cd(II) on both the two resins is favorable.

Based on the above analysis, the authors assume that the adsorption of Cd(II) ion by resins proceeds via several stages: the transfer of Cd(II) ions from the bulk solution to the liquid-solid interface (occurs very quickly); the diffusion of Cd(II) ions through the boundary layer that surrounds the resin particles (the rate-determining step); the diffusion of Cd(II) ions from the surface to the interior of the resin particles; and the adsorption of Cd(II) ions to the active sites on the resin surface (occurs very quickly) (Malamis & Katsoua

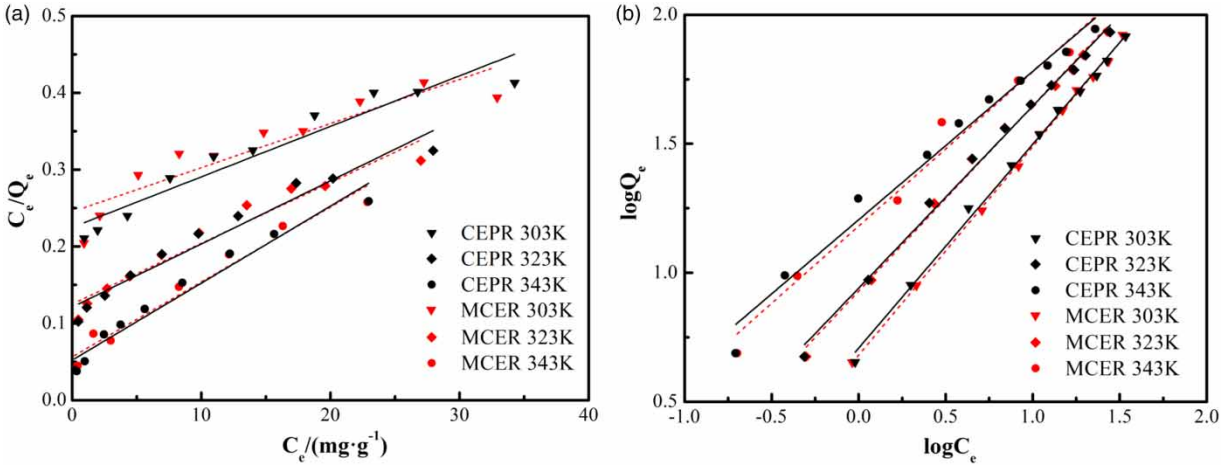

Figure 8 | Adsorption isotherm of Cd(II) on CEPR and MCER: (a) Langmuir, (b) Freundlich.

2013). The driving forces for adsorption include physical and chemical factors such as the concentration difference of Cd(II) between the solution and the interior of the resin, electrostatic attraction between the Cd(II) ions and the electronegative areas ($-SO_3^-$ and TAIC moieties) of the resins (at a very close range), ion exchange, and van der Waals forces. Therefore, the adsorption of Cd(II) on the MCER could be a combined effect of both chemisorption and physisorption, with ion exchange as the main process.

Previous literature reported that SDS-modified chitosan beads (Pal & Pal 2017) and EDTA-modified maghemite microspheres (mag-ligands) (Huang & Keller 2015) were used as adsorbents to remove Cd(II) from wastewater. The adsorption capacity of Cd(II) was 125 mg/g for the SDS-modified chitosan beads and 79.41 mg/g for the mag-ligand. Both adsorbents exhibited better adsorption efficiency of Cd(II) than the MCER and CEPR prepared in present study. The adsorption of Cd(II) on the chitosan beads was attributed to the enhanced electrostatic attraction, while the adsorption on the mag-ligands was attributed to the complexation reactions with EDTA and physical adsorption on the surface porous structures. Other adsorbents such as activated carbons (Nadeem *et al.* 2009), functional graphene oxide (Bian *et al.* 2015) and lignin-based ion-exchange resin (Liang *et al.* 2013) were developed to adsorb Cd(II) from wastewater, but exhibited an ordinary-level adsorption for Cd(II), likely owing to the lack of functional groups and active sites. As a whole, magnetic adsorbents such as the mag-ligands and the MCER prepared in our study have the potential for broad industrial applications due to the following advantages: easily separated after adsorption, easily recovered, regenerated and reused, significantly increasing treatment efficiency and reducing operation cost.

Regeneration of cation-exchange resins

The usefulness of an adsorbent in the adsorption process depends not only on the adsorptive capacity but also on how well the adsorbent can be regenerated and used again. The regeneration and reuse of adsorbents is a formidable challenge for their widespread application. Figure 9

Table 3 | Adsorption parameters of Langmuir and Freundlich isotherm models for Cd(II) adsorption on the two resins

			Langmuir			Freundlich		
Resins	**T (K)**	**Q_{exp}**	**b**	**Q_m**	**R^2**	**K_F**	**1/n**	**R^2**
CEPR	303	43.19	0.0292	151.97	0.9180	5.119	0.790	0.9963
	323	45.09	0.0676	121.65	0.9524	8.740	0.705	0.9936
	343	47.01	0.1910	99.70	0.9583	16.108	0.575	0.9791
MCER	303	43.19	0.0234	174.22	0.8345	4.791	0.808	0.9988
	323	45.11	0.0628	126.58	0.9412	8.490	0.718	0.9949
	343	47.02	0.1713	102.56	0.9598	15.212	0.598	0.9772

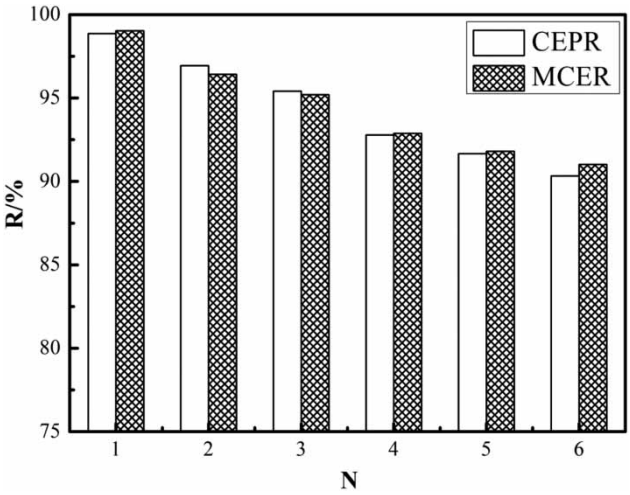

Figure 9 | Desorption-adsorption cycle efficiency (R) for CEPR and MCER with Cd(II) ion.

shows the adsorption-desorption cycle efficiency of the two resins for the Cd(II) ion after each adsorption-desorption cycle. Even after six cycles, the CEPR and MCER still exhibit high adsorption efficiencies (higher than 90%), indicating that the two resins can be regenerated with a low-concentration HCl solution and have good reusability. The MCER can be easily recovered from wastewater by applying an external magnetic field, suggesting its potential for application in the treatment of actual Cd(II) wastewater.

CONCLUSIONS

In this study, magnetic and non-magnetic cation-exchange polystyrene resins were developed in a stainless steel reactor and used for the removal of Cd(II) ions from aqueous solutions. Structural and morphological analyses revealed that the two resins had higher specific surface area, and were mesoporous microspheres. MCER contained about 25% Fe_3O_4 and exhibited a high magnetic response. The two resins could remove Cd(II) ions efficiently from the simulated Cd solution. The adsorption processes attained equilibrium within 120 min for the MCER and 300 min for the CEPR, and are well described by a pseudo-second-order kinetic model. Furthermore, the equilibrium adsorption data fitted the Freundlich isotherm model better than the Langmuir model, indicating that the adsorption of Cd(II) by the two resins was mostly ion-exchange adsorption. The superior magnetic response and regeneration of the MCER make it a good candidate as an adsorbent for removing Cd(II) from wastewater.

ACKNOWLEDGEMENTS

The authors are grateful for support from the National Natural Science Foundation of China (Nos 21566004 and 21266002), the Guangxi Natural Science Foundation (2015GXNSFAA139036) and the Scientific Research Foundation of Guangxi University (Nos XGZ120081 and XTZ140787).

REFERENCES

Bagheri, H., Afkhami, A., Saber-Tehrani, M. & Khoshsafar, H. 2012 Preparation and characterization of magnetic nanocomposite of Schiff base/silica/magnetite as a preconcentration phase for the trace determination of heavy metal ions in water, food and biological samples using atomic absorption spectrometry. *Talanta* **97**, 87–95.

Barakat, M. A. 2011 New trends in removing heavy metals from industrial wastewater. *Arabian Journal of Chemistry* **4**, 361–377.

Barton, J., García, M. B. G., Santos, D. H., Fanjul-Bolado, P., Ribotti, A., McCaul, M., Diamon, D. & Magni, P. 2016 Screen-printed electrodes for environmental monitoring of heavy metal ions: a review. *Microchimica Acta* **183**, 503–517.

Bazargan, A., Shek, T. H., Hui, C. W. & Mckay, G. 2017 Optimising batch adsorbers for the removal of zinc from effluents using a sodium diimidoacetate ion exchange resin. *Adsorption* **23**, 477–489.

Benbrahim-Tallaa, L., Tokar, E. J., Diwan, B. A., Dill, A. L., Coppin, J. F. & Waalkes, M. P. 2009 Cadmium malignantly transforms normal human breast epithelial cells into a basal-like phenotype. *Environmental Health Perspectives* **117**, 1847–1852.

Bhatt, R. R., Shah, B. A. & Shah, A. V. 2012 Uptake of heavy metal ions by chelating ion-exchange resin derived from p-hydroxybenzoic acid-formaldehyde-resorcinol: synthesis, characterization and sorption dynamics. *The Malaysian Journal of Analytical Sciences* **16**, 117–133.

Bian, Y., Bian, Z. Y., Zhang, J. X., Ding, A. Z., Liu, S. L. & Wang, H. 2015 Effect of the oxygen-containing functional group of graphene oxide on the aqueous cadmium ions removal. *Applied Surface Science* **329**, 269–275.

Chen, X. 2015 Modeling of experimental adsorption isotherm data. *Information* **6**, 14–22.

Davarpanah, M., Ahmadpour, A. & Bastami, T. R. 2015 Preparation and characterization of anion exchange resin decorated with magnetite nanoparticles for removal of *p*-toluic acid from aqueous solution. *Journal of Magnetism and Magnetic Materials* **375**, 177–183.

Farnad, N., Farhadi, K. & Voelcker, N. H. 2012 Polydopamine nanoparticles as a new and highly selective biosorbent for the removal of copper (II) ions from aqueous solutions. *Water Air and Soil Pollution* **223**, 3535–3544.

Fu, F. L. & Wang, Q. 2011 Removal of heavy metal ions from wastewaters: a review. *Journal of Environmental Management* **92**, 407–418.

Fu, Y., Zhao, J., Wang, Q. & Wan, L. 2016 Adsorption efficiency of lignin-based ion exchange resin on heavy metal ions. *Chinese Journal of Environmental Engineering* **10**, 4314–4318.

Guo, L., Zhang, J., Zhang, D., Liu, Y., Deng, Y. & Chen, J. 2012 Preparation of poly(vinylidene fluoride-co-tetrafluoroethylene)-based polymer inclusion membrane using bifunctional ionic liquid extractant for Cr(VI) transport. *Industrial and Engineering Chemistry Research* **51**, 2714–2722.

Huang, Y. & Keller, A. A. 2015 EDTA functionalized magnetic nanoparticle sorbents for cadmium and lead contaminated water treatment. *Water Research* **80**, 159–168.

Järup, L. 2003 Hazards of heavy metal contamination. *British Medical Bulletin* **68**, 167–182.

Kara, A., Demirbel, E., Tekin, N., Osman, B. & Besirli, N. 2015 Magnetic vinylphenylboronic acid microparticles for Cr (VI) adsorption: kinetic, isotherm and thermodynamic studies. *Journal of Hazardous Materials* **286**, 612–623.

Khambhaty, Y., Mody, K., Basha, S. & Jha, B. 2009 Kinetics, equilibrium and thermodynamic studies on biosorption of hexavalent chromium by dead fungal biomass of marine *Aspergillus niger*. *Chemical Engineering Journal* **145**, 489–495.

Lee, Y., Rho, J. & Jung, B. 2010 Preparation of magnetic ion-exchange resins by the suspension polymerization of styrene with magnetite. *Journal of Applied Polymer Science* **89**, 2058–2067.

Li, K., Li, P., Cai, J., Xiao, S., Yang, H. & Li, A. 2016 Efficient adsorption of both methyl orange and chromium from their aqueous mixtures using a quaternary ammonium salt modified chitosan magnetic composite adsorbent. *Chemosphere* **154**, 310–318.

Li, Q., Fu, L., Wang, Z., Li, A., Shuang, C. & Gao, C. 2017 Synthesis and characterization of a novel magnetic cation exchange resin and its application for efficient removal of Cu^{2+} and Ni^{2+} from aqueous solutions. *Journal of Cleaner Production* **165**, 801–810.

Liang, F. B., Song, Y. L., Huang, C. P., Li, Y. X. & Chen, B. H. 2013 Synthesis of novel lignin-based ion-exchange resin and its utilization in heavy metals removal. *Industrial and Engineering Chemistry Research* **52**, 1267–1274.

Malamis, S. & Katsoua, E. 2013 A review on zinc and nickel adsorption on natural and modified zeolite, bentonite and vermiculite: examination of process parameters, kinetics and isotherms. *Journal of Hazardous Materials* **252–253**, 428–461.

Martinez, G. V. F., Torres, J. R. P., García, J. L. V., Munive, G. C. T. & Zamarripa, G. G. 2012 Kinetic aspects of gold and silver recovery in cementation with zinc power and electrocoagulation iron process. *Advances in Chemical Engineering and Science* **2**, 342–349.

Millar, G. J., Miller, G. L., Couperthwaite, S. J. & Papworth, S. 2016 Factors influencing kinetic and equilibrium behaviour of sodium ion exchange with strong acid cation resin. *Separation and Purification Technology* **163**, 79–91.

Morales, M. E., Derbes, R. S., Ade, C. M., Ortego, J. C., Stark, J., Deininger, P. L. & Roy-Engel, A. M. 2016 Heavy metal exposure influences double strand break DNA repair outcomes. *PLoS One* **11**, e0151367.

Nadeem, M., Shabbir, M., Abdullah, M. A., Shah, S. S. & Mckay, G. 2009 Sorption of cadmium from aqueous solution by surfactant-modified carbon adsorbents. *Chemical Engineering Journal* **148**, 365–370.

Naser, H. A. 2013 Assessment and management of heavy metal pollution in the marine environment of the Arabian Gulf: a review. *Marine Pollution Bulletin* **72**, 6–13.

Pal, P. & Pal, A. 2017 Surfactant-modified chitosan beads for cadmium ion adsorption. *International Journal of Biological Macromolecules* **104**, 1548–1555.

Pan, S. D., Shen, H. Y., Xu, Q. H., Luo, J. & Hu, M. Q. 2012 Surface mercapto engineered magnetic Fe_3O_4 nanoadsorbent for the removal of mercury from aqueous solutions. *Journal of Colloid and Interface Science* **365**, 204–212.

Plazinski, W., Dziuba, J. & Rudzinski, W. 2013 Modeling of sorption kinetics: the pseudo-second order equation and the sorbate intraparticle diffusivity. *Adsorption* **19**, 1055–1064.

Shen, H., Chen, J., Dai, H., Wang, L. & Hu, M. 2013 New insights into the sorption and detoxification of chromium (VI) by tetraethylenepentamine functionalized nanosized magnetic polymer adsorbents: mechanism and pH effect. *Industrial and Engineering Chemistry Research* **52**, 12723–12732.

Tao, P., Shao, M., Song, C., Wu, S., Cheng, M. & Cui, Z. 2014 Preparation of porous and hollow Mn_2O_3 microspheres and their adsorption studies on heavy metal ions from aqueous solutions. *Journal of Industrial and Engineering Chemistry* **20**, 3128–3133.

Wong, C. W., Barford, J. P., Chen, G. & Mckay, G. 2014 Kinetics and equilibrium studies for the removal of cadmium ions by ion exchange resin. *Journal of Environmental Chemical Engineering* **2**, 698–707.

Wu, F. C., Tseng, R. L. & Juang, R. S. 2009 Initial behavior of intraparticle diffusion model used in the description of adsorption kinetics. *Chemical Engineering Journal* **153**, 1–8.

Yu, J., Chi, R., Zhang, Y., Xu, Z., Xiao, C. & Guo, J. 2012 A situ co-precipitation method to prepare magnetic PMDA modified sugarcane bagasse and its application for competitive adsorption of methylene blue and basic magenta. *Bioresource Technology* **110**, 160–166.

First received 8 January 2018; accepted in revised form 17 May 2018. Available online 31 May 2018